THEOPOLD, K. H., BECKER, P. N. & BERGMAN, R. G. (1982). *J. Am. Chem. Soc.* **104**, 5250–5252.
TRANQUI, D., DURIF, A., NASR EDDINE, M., LIETO, J., RAFALKO, J. J. & GATES, B. C. (1982). *Acta Cryst.* B**38**, 1916–1920.
TULINSKY, A. & VAN DER HENDE, J. H. (1967). *J. Am. Chem. Soc.* **89**, 2905–2911.
VENABLE, T. L., SINN, E. & GRIMES, R. N. (1982). *Inorg. Chem.* **21**, 895–904.
WEBER, D., MUJICA, C. & VON SCHNERING, H. G. (1982). *Angew. Chem. Suppl.* pp. 1801–1812.
YAMADA, K., TAKEDA, M., ITOH, N., UMINO, N., IZEKAWA, A., KIYOMOTO, A., AOE, K., KOTERA, K. & IWAKUMA, T. (1982). *Chem. Pharm. Bull.* **30**, 1588–1593.

Acta Cryst. (1984). A**40**, 668-675

Anharmonic Potentials and Pseudo Potentials in Ordered and Disordered Crystals

BY ROLF BACHMANN AND HEINZ SCHULZ

Max-Planck-Institut für Festkörperforschung, Heisenbergstrasse 1, 7000 *Stuttgart* 80,
Federal Republic of Germany

(*Received* 27 *January* 1984; *accepted* 18 *May* 1984)

Abstract

An extension of existing structure-factor formalisms for anharmonic thermal motion in crystals and the corresponding one-particle potentials is presented and applied to ordered and disordered structures. A generalized probability density function (joint p.d.f.) is introduced and it is first shown that anharmonic temperature factors ('thermal motion') and split positions ('disorder') are mathematically equivalent in describing electron or nuclear densities. When probability densities are interpreted in terms of an effective one-particle potential, however, ordered and disordered structures show different behaviour. For ordered structures the effective one-particle potentials are found to be almost independent of temperature; for disordered structures one obtains a temperature-dependent pseudo potential. The different temperature dependence can be used to distinguish between order and disorder. Pseudo potentials are calculated for several types of disorder and compared with potentials derived from X-ray or neutron diffraction experiments.

Introduction

Anharmonic thermal motion of atoms (or ions) in crystals can be studied with the aid of accurate elastic X-ray or neutron diffraction. The measured intensities contain information about the average distribution of atoms around their equilibrium positions (*i.e.* the probability density function p.d.f.) and allow the determination of the effective one-particle potential (OPP) in which the atoms are moving (Dawson, Hurley & Maslen, 1967; Willis, 1969; Willis & Pryor, 1975; Mair, 1980; Zucker & Schulz, 1982*a*).

A particularly interesting group of materials with high anharmonic thermal motion is formed by ionic conductors, which have been extensively studied in recent years [*e.g.* AgI (Cava, Reidinger & Wuensch, 1977), Li_3N (Zucker & Schulz, 1982*b*), Ag_3SI (Perenthaler, Schulz & Beyerle, 1981), $RbAg_4I_5$ (Kuhs, 1983)]. The OPPs allow estimation of the potential barrier for ionic motion and it compares well with the activation energy of conductivity. Thus one has for this special type of material another experimental test for the potential derived from a diffraction experiment.

For some ionic conductors, however, we found a great difference between the activation energy and, in addition, a strongly temperature dependent potential. This result cannot be understood using the usual concepts of a p.d.f. and the corresponding OPP. The necessary extensions of these concepts include the effects of disorder and will be presented hereafter.

The joint probability density function (PDF)

For an isolated atom vibrating around a given equilibrium position, the one-particle p.d.f. is the average in space and time of the probability of finding the atom in a volume element around its equilibrium position. The p.d.f. is then the Fourier transform of the temperature factors (harmonic or anharmonic) associated with this position which are obtained from the measured intensities (Willis, 1969; Johnson & Levy, 1974). This definition of the p.d.f. is only meaningful if different p.d.f.s do not overlap so that electron or nuclear densities can uniquely be assigned to one position, *i.e.* if the p.d.f.s are immeasurably small between two positions.

In some cases the amplitudes of thermal motion become comparable with the distance between two positions. Examples are ionic conductors with a continuous distribution of mobile ions along the conduction path and disordered structures with split positions. This leads to densities between different positions which cannot be unambiguously assigned to one position, and single positions then overlap. The sum of all contributions of single p.d.f.s, however, is unique and we therefore introduce the joint probability density function (PDF) which is given by the following formula:

$$\mathrm{PDF}_k(\mathbf{r}) = \textstyle\sum_i w_{ik}\,\mathrm{pdf}_{ik}(\mathbf{r}); \tag{1}$$

k is the type of atom, w_{ik} is the occupancy of position i by an atom type k, and the sum $\sum_i$ is taken over all positions that can be occupied by atoms of type k. PDF_k is the probability of finding an atom of type k in a volume element of the crystal. Its integral over one unit cell is equal to the number of atoms of type k per unit cell (the integral for each p.d.f. is equal to 1). [The program *MULPDF* was written to calculate the joint-p.d.f. This program is obtainable as part of the program system *PROMETHEUS* (Zucker, Perenthaler, Kuhs, Bachmann & Schulz, 1983)].

The ambiguity in determining single p.d.f.s leads to high correlations between positional and thermal parameters of different positions during the refinement and the errors on these parameters are rather high. The PDF, however, is not affected by these correlations and can be accurately determined.

As for single p.d.f.s, the physical significance of the joint p.d.f. has to be checked throughout the refinement. Large negative values of a p.d.f. are meaningless and show that the present model is wrong. In some cases the PDF is still positive although the single p.d.f.s have large negative regions. In this case the negative regions of the single p.d.f.s have no significance and merely reflect the fact that, in the case of overlap, single p.d.f.s cannot be uniquely determined.

The PDF is closely related to the partial Fourier densities obtained from neutron data. Although the PDF can only be calculated with the aid of a model, it has many advantages compared with Fourier densities:

(1) It can be derived from a limited data set because it is the density of a model fitted to measured data. (Accuracy and resolution are, of course, not higher than those of a Fourier density. With a few reflections missing, however, Fourier densities are no longer interpretable.)

(2) It is not affected by termination effects, such as termination ripples.

(3) The Fourier transform of the temperature factors is analytical.

(4) Quasi nuclear densities can be derived from X-ray data.

Apart from its original use, the joint p.d.f. provides a convenient method of extending any given formalism which can describe anharmonic distributions. The superposition of p.d.f.s weighted with the corresponding occupancy can be viewed as another way to write down an expansion (Appendix 1). Instead of introducing anharmonic parameters of higher order, one can introduce extra positions in the refinement (Mair, 1982*a*). These extra positions are not equilibrium positions that can be occupied by an atom, but merely a mathematical aid. This 'expansion', however, is not unique (Appendix 1). Furthermore, each extra position can be refined anharmonically. This opens a wide variety of different ways to describe the same joint p.d.f.

Not only can anharmonic temperature factors be described by extra positions, but conversely the joint p.d.f. of split positions, where different positions lie close together, can be described by anharmonic temperature factors. This demonstrates that one cannot distinguish between ordered and disordered structures with just one data set measured at only one temperature.

Since the description of a p.d.f. with extra positions is not unique, one often encounters high correlations during the refinement of split positions; in this case the refinement of anharmonic temperature factors is usually easier. Extra positions have to be used, however, if the highest anharmonic order one can refine proves to be insufficient. For example, sixth-order anharmonic temperature factors were not sufficient for the description of the fluorine distribution in β-lead fluoride at high temperatures (Bachmann & Schulz, 1983). The continuous distribution of mobile ions in ionic conductors can only be described with the aid of several positions which may be symmetrically equivalent.

As an example of an experimental PDF we present the distribution of the silver ions in the β phase of $\mathrm{Ag_3SI}$. This phase is cubic (space group $Pm3m$) with sulphur and iodine occupying the centre and corners of the cube and silver occupying positions near the centre of the cube faces. From the refined structure parameters of Perenthaler (1981) and Perenthaler, Schulz & Beyerle (1981), we calculated the PDF of the silver ions at 493K (Fig. 1). The PDF shows the conduction path which could not be obtained from single p.d.f.s or difference Fourier maps.

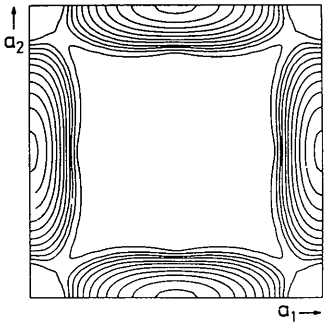

Fig. 1. Joint p.d.f. of silver in β-$\mathrm{Ag_3SI}$ at 493 K in the {200} planes. Contour lines: 0·5, 1, 2, 4, 8, 16, 32, 64, 128, 256, 512 Å^{-3}.

Perenthaler *et al.* (1981) have already refined two models for the silver distribution: one model with one silver position at the face centre $\{1/2, 1/2, 0\}$ and anharmonic temperature factors up to sixth order and a second model with four split positions (atomic positions $1/2, x, 0\}$ $x \simeq \cdot 45$) and anharmonic temperature factors up to third order. For low temperatures they obtained a slightly better fit with the split model (ratio of R_ws* ranging between 1.05 and 1.1), for higher temperatures the anharmonic model was better (ratio of R_ws between 0.92 and 0.65). A comparison of the PDF's of both models (see Fig. 2) shows that they are very similar, demonstrating the (mathematical) equivalence of the two models.

The effective one-particle potential

The effective one-particle potential is an average potential energy of an atom caused by the interaction with all the other atoms of the crystal. The time average over all possible configurations of the other atoms leads to a potential that depends only on the position of one atom.

In the classical regime (at temperatures above the Debye temperature), the effective one-particle potential of an isolated atom is related to the p.d.f. by the following formula (Willis, 1969):

$$V(\mathbf{r}) = V_0 - kT \ln[\mathrm{pdf}(\mathbf{r})], \tag{2}$$

k is the Boltzmann constant, T is the absolute temperature.

Forumula 2 is now extended to the joint p.d.f. This extension is straightforward if anharmonic thermal vibrations are artificially described by additional positions. In this case the joint p.d.f. is only a way to write down an expansion and has the same physical meaning as a single p.d.f. The potential remains the effective one-particle potential for isolated atoms. Potentials from single p.d.f.s have no physical meaning in this case because the extra positions are a mathematical aid.

In all other cases, the potential defined by the joint p.d.f. and (2) is no longer the potential of an isolated atom. For the interpretation of this potential one has to distinguish between ordered structures (dynamic disorder due to thermal vibrations only) and disordered structures (in addition to thermal vibrations, static deviations from the crystal symmetry).

Ordered structures

For ordered structures, the effective one-particle potential derived from the joint p.d.f. is very similar to the usual effective one-particle potential. For regions where the single p.d.f.s do not overlap, the potential of the joint p.d.f. is, apart from the arbitrary constant V_0, equal to the potentials of the single p.d.f.s. Where single p.d.f.s do overlap, the joint p.d.f. gives a unique value for the potential.

One can now determine the potential along the conduction path of an ionic conductor and calculate the potential barrier. A good example is lithium nitride (Li_3N). It is a nearly ordered fast ion conductor, with defect concentrations below 2% (Zucker & Schulz, 1982*b*; Bell, Breitschwerdt & Van Alpen, 1981). The potentials calculated from single p.d.f.s and the joint p.d.f. are shown together in Fig. 3. The two potentials are equal in the region where single p.d.f.s do not overlap; near the potential barrier, where they overlap, the single p.d.f.s give values which are too high (*e.g.* 0·32 eV at the potential barrier). The potential barrier obtained with the joint p.d.f., however, has a value of 0·27(3) eV which is very close to the activation energy of conductivity of 0·25(2) eV (Bell *et al.*, 1981).

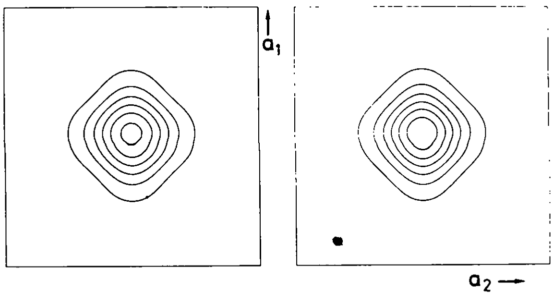

(*a*) (*b*)

Fig. 2. Distribution of silver in β-Ag_3SI at 493 K in the {100} planes. Contour lines: 16, 32, 64, 128, 256, 512 Å^{-3}. (*a*) PDF from four split positions [atomic positions (0·5, ± *x*, 0), (± *x*, 0·5, 0), $x \simeq 0{\cdot}45$]. Split positions were refined with third-order temperature factors. (*b*) P.d.f. from one position at (0·5, 0·5, 0) refined with temperature factors up to sixth order.

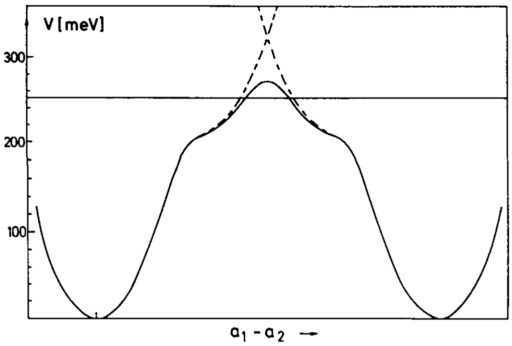

Fig. 3. Effective one-particle potential of the Li(2) ions in Li_3N along the conduction path (direction [1$\bar{1}$0]) at $T = 888$ K. The straight line indicates the activation energy of conductivity. Solid line: potential from the joint p.d.f. Broken line: Potentials from single p.d.f.s.

$$* \; R_w = \frac{\sum w(F_{\mathrm{obs}} - F_{\mathrm{calc}})^2}{\sum w F_{\mathrm{obs}}^2}.$$

Disordered structures

For disordered structures the content of some unit cells differs from the content of other unit cells. Elastic diffraction data, however, give only the average content of all unit cells and p.d.f.s that are the average over the different p.d.f.s of all unit cells. Because of this spatial average, the potential derived from the diffraction experiment does not give the average potential energy of the ions, but it is a pseudo potential which is broader than the real average potential. The form of the pseudo potential and its temperature dependence is different for the case that the positions can be resolved in a Fourier transform of the p.d.f. map or the case that some positions are so close together compared with the thermal vibrations that the average p.d.f. has only one maximum.

The pseudo potential in the case of resolved positions

It should be noted that, in this case, it is possible to determine the potential difference between symmetrically inequivalent sites. If all sites are underoccupied, the occupation of each position will adjust itself according to the potential difference and the temperature. The potential difference between two sites is then given by

$$V(\mathbf{x}_1) - V(\mathbf{x}_2) = -kT \ln\left[w_1 \mathrm{pdf}_1(\mathbf{x}_1)/w_2 \mathrm{pdf}_2(\mathbf{x}_2)\right]. \tag{3}$$

One has to take into account, however, the limited accuracy of single p.d.f.s where they overlap.

The pseudo potential was calculated for a simple model consisting of two types of one-dimensional chains which overlap in the averaged structure. The potential was assumed to be sinusoidal in each chain and the arrangement of atoms within one chain to be ordered. The atomic positions in half of the chains were at 0·25 {corresponding to a potential $V_1 = V_0 \cos[2\pi(x/a - 0{\cdot}25)]$ and at 0·75 ($V_2 = V_0 \cos[2\pi(x/a - 0{\cdot}75)]$} in the other chains (Fig. 4*a*). (One could also assume only local order within one chain over a few unit cells. The averaging process would then be over different parts of one chain instead of over different chains). The pseudo potential was then obtained from the joint p.d.f. of the averaged structure using (2).

The pseudo potential is shown in Fig. 4(*b*). At low temperatures the densities remain concentrated near the potential minima and at points where the density is very large in one chain it is very low in the other chain. The pseudo potential near 0·25 is very close to the potential in the first chain and the pseudo potential near 0·75 very close to the potential in the second chain. One can therefore obtain the potential of either chain near the potential minima, but one cannot follow this potential very far and, in particular, it is impossible to determine the density in one chain at the potential barrier for a motion along this chain; the apparent potential barrier of the pseudo potential is much too low (for this model the factor is 1/2 or less).

With increasing temperature the pseudo potential becomes flatter and less information can be obtained from it. The distribution in one chain and near a potential minimum is approximated by the single p.d.f. which can therefore be used to estimate the potential in a chain.

An example of this case is the high-temperature phase of CuTeBr, a very anisotropic ionic conductor with a preferred one-dimensional conduction along the *c* axis (Bachmann, Kreuer, Rabenau & Schulz, 1982). The mobile ions are arranged in chains parallel to the *c* axis; the arrangement of the ions, however, is different for different chains. In the averaged structure, densities of different chains overlap in a very similar way to that described in the model above. A great difference had been found between the activation energy of conductivity (0.25eV) and the potential barrier obtained from the joint p.d.f. (0·10 eV) or from a connection of the potentials of single p.d.f.s (0·13 eV, Fig. 5). This difference can now be explained by the averaging of densities of different chains obtained in the diffraction experiment.

In three dimensions the situation is, in principle, the same if one substitutes the different chains by different ordered regions.

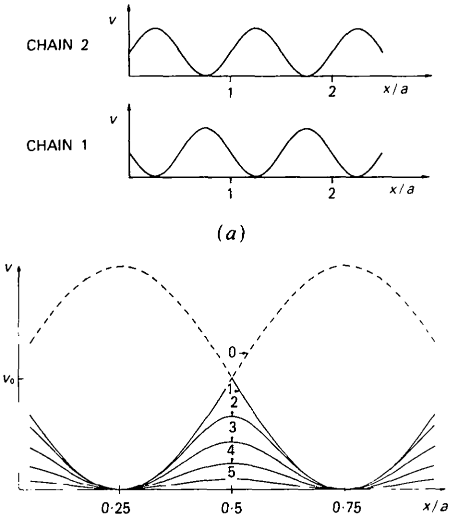

(*b*)

Fig. 4. (*a*) Potential within the different types of chains. (*b*) Pseudo potential for the averaged structure: (0) the broken line indicates the real potential in each chain; (1) $T = 0$ K; (2) $V_0/kT = 2$; (3) $V_0/kT = 1$; (4) $V_0/kT = 0.5$; (5) $V_0/kT = 0{\cdot}2$. V_0 is the maximum potential barrier that can be derived in a diffraction experiment for this model.

Unresolved split positions

For split positions, the distances between different positions become comparable to the vibrational amplitudes of the atoms so that a single position cannot be resolved as a separate maximum in a Fourier transform or p.d.f. map.

The pseudo potential was calculated for a simple split model as a function of temperature as shown in Fig. 6. The split model has two positions. The potential of an atom at either position is assumed to be harmonic and independent of temperature. The pseudo potential is again obtained from the joint p.d.f. of the averaged structure.

The pseudo potential shows a strong temperature dependence. At low temperatures (compared with the potential energy of an atom midway between the two positions V_b) the pseudo potential shows a maximum between the two positions. This maximum decreases with increasing temperature very similar to the case considered above. At $T = V_b/k \ln 2$, however, this maximum vanishes and the pseudo potential has only one minimum which is very flat. With still increasing temperature, the pseudo potential becomes steeper and finally, as the temperature goes to infinity, it assumes the same form as the original potential in which an atom at one of the positions is moving (Appendix 2).

This behaviour of the pseudo potential is characteristic for all split models. A resolution of a single position is only possible at temperatures below $T = V_b/k \ln(n)$, where n is the number of split positions. At high temperatures the static displacements of the split positions from their centre of gravity become less and less important compared with the thermal vibrations, and the pseudo potential with a minimum at the centre of gravity begins to resemble more and more the real potential at one of the split positions (Appendix 2).

The static displacements of split positions add a constant term to the harmonic coefficients of the temperature factors if the split positions are refined from the centre of gravity (Megaw, 1969; Schulz, 1972). Extrapolating back to 0 K these coefficients give the average displacement of split positions from the centre of gravity. This is also true for anharmonic descriptions of the p.d.f. if the Edgeworth or the Gram–Charlier series (Johnson, 1970; Johnson & Levy, 1974) is used (Appendix 3).

An example of split positions is the distribution of sodium ions in Na β-alumina around the Beevers–Ross site. The structure of Na β-alumina is built up of spinel blocks separated by planes. These planes, in which the sodium ions can diffuse, have two different sodium sites: the so-called Beevers-Ross site and the mid-oxygen site. A structure analysis at 80 K (Reidinger, 1979) revealed that the sodium ions near the Beevers–Ross site are distributed over three split positions. The Fourier map showed three separate maxima near this site which did not appear at higher temperatures.

The potential of the sodium ions between 298 and 913 K obtained from another structure investigation (Bachmann, 1983) is shown in Fig. 7. The lowest minimum corresponds to the Beevers–Ross site (the split positions are not resolved in this temperature range), the second minimum to the mid-oxygen site.

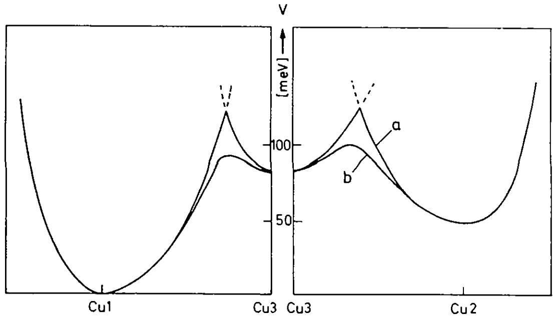

Fig. 5. (*a*) Potential of copper ions in CuTeBr obtained by connecting potentials of single p.d.f.s. The conduction path in CuTeBr connects sites Cu(1) and Cu(2) *via* Cu(3). The left side of the figure shows the potential in the direction Cu(1)–Cu(3), the right part in the direction Cu(3)–Cu(2). (*b*) Pseudo potential obtained from the joint p.d.f. at 473 K.

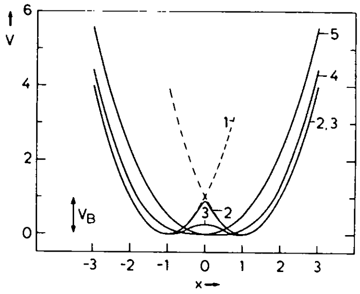

Fig. 6. Pseudo potential for two split positions at $x_0 = -1$ and $x_0 = 1$. Potential at each position: $V = V_b(x - x_0)^2$. (1) $T = 0$ K; (2) $V_b/kT = 10$; (3) $V_b/kT = 1$; (4) $V_b/kT = 0{\cdot}5$; (5) $V_b/kT = 0{\cdot}25$.

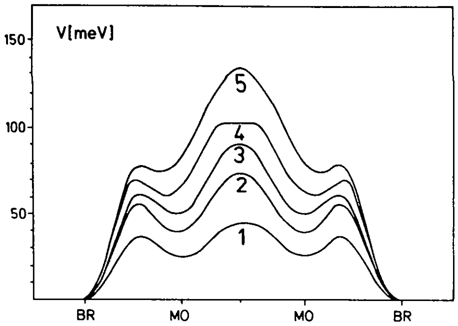

Fig. 7. Pseudo potential in Na β-alumina along the conduction path. BR: Beevers–Ross site, MO: mid-oxygen site. Temperatures: (1) 295 K; (2) 450 K; (3) 620 K; (4) 770 K; (5) 910 K.

The potential near the Beevers–Ross site becomes steeper with increasing temperature and the potential difference between the two sites seems to increase, thus showing the typical behaviour of a pseudo potential in the case of split positions. The temperature dependence of the potential near the mid-oxygen site and the potential barrier is much smaller than the temperature dependence near the Beevers–Ross site. The apparent height of the potential barrier, the difference between the potential at the Beevers–Ross site and the highest potential along the conduction path, increases with increasing temperature from 45 to 135 meV. The latter value is already very close to the activation energy of conductivity (0·17 eV) (Wittingham & Huggins, 1971).

Distinguishing between order and disorder

If all positions are well separated they can be resolved in Fourier or PDF maps. Disorder is then exhibited by an underoccupation of sites or by interatomic distances which are too short for simultaneous occupation.

The situation is more difficult for unresolved split positions which have only one maximum in Fourier or PDF maps even for an unlimited data set.

A high static harmonic temperature factor in an extrapolation to 0 K is a first indication of split positions. This method, however, is not always reliable. Since a set of parameters describing a point p.d.f. is not unique the exact value of the harmonic parameter may not be known. Furthermore, some anharmonic potentials also lead to a 'static' temperature factor in an extrapolation to 0 K (Mair, 1982*b*; Appendix 3).

The strong temperature dependence of the pseudo potential is therefore a better way to detect unresolved split positions. Contrary to the pseudo potential of split positions, the potential in ordered crystals is, apart from small effects due to thermal expansion, found to be independent of temperature as long as the temperature is not close to a phase transition (see *e.g.* Mair, Barnea, Cooper & Rouse, 1974; Roberto, Battermann & Keating, 1974; Zucker & Schulz, 1982*b*). Although this behaviour is generally obeyed by most materials, there are exceptions where the potential changes with temperature, such as materials with an unusual phonon temperature dependence, or ionic conductors, where the conductivity deviates from the Arrhenius law. To distinguish then between order and disorder one has to compare the actual change of the potential (*e.g.* the temperature dependence of the activation energy) with the temperature dependence of the potential derived from X-ray or neutron diffraction experiments.

One of us (RB) gratefully acknowledges the support of a Krupp doctoral fellowship.

APPENDIX 1

Expansion of a p.d.f. by extra positions

Introducing extra positions to describe a p.d.f. means one describes the p.d.f. as a sum of functions which (in one dimension) have the following form:

$$h(x) = a \exp[-b(x-x_0)^2],$$

where the occupancy a, the temperature factor b and the position x_0 have to be determined by refinement.

The functions

$$\begin{aligned} g_n(x) &= \exp[-b(x-n)^2] \\ &= \exp[-b(x^2+n^2)][\exp(2bx)]^n \end{aligned}$$

with b fixed and n a positive integer already form a complete set of functions as can be seen by comparison with the functions u^n and substituting

$$u = \exp(2bx).$$

This proves that any p.d.f. can be described by additional positions. Because of the freedom in choosing temperature factors and positions one has more functions available than are necessary. Hence the temperature factors and positions cannot be unambiguously determined.

APPENDIX 2

The pseudo potential of unresolved split positions at high temperatures

First the harmonic case is considered. Each split position $\mathbf{x}_i$ has an occupancy c_i with $\sum_i c_i \mathbf{x}_i = 0$ and $\sum_i c_i = 1$. The potential at each position is assumed to have the same form.

(a) The potential at different positions is given by a translation

$$V_i(\mathbf{x}) = V_0(\mathbf{x}-\mathbf{x}_i) = (\mathbf{x}-\mathbf{x}_i)B(\mathbf{x}-\mathbf{x}_i).$$

The pseudo potential is then given by

$$\begin{aligned} PV(x) &= C - kT \ln \sum_i c_i \exp[-(\mathbf{x}-\mathbf{x}_i)B(\mathbf{x}-\mathbf{x}_i)/kT] \\ &= C - kT \ln \sum_i c_i \exp[f_i(\bar{\mathbf{x}}-\bar{\mathbf{x}}_i)/kT]. \end{aligned}$$

The limit $T \to \infty$ gives

$$\begin{aligned} PV(x) &= C + \sum_i c_i f_i(\mathbf{x}-\mathbf{x}_i) \\ &= C + \sum_i c_i(\mathbf{x}B\mathbf{x} - 2\mathbf{x}\mathbf{B}\mathbf{x}_i + \mathbf{x}_i B\mathbf{x}_i) \\ &= C + \mathbf{x}B\mathbf{x} - 2\mathbf{x}B(\sum_i c_i\mathbf{x}_i) + \sum_i c_i\mathbf{x}_i B\mathbf{x}_i \\ &= C' + \mathbf{x}B\mathbf{x} \end{aligned}$$

so that the pseudo potential assumes the same form as each of the potentials at a split position.

(*b*) In general the transformation from one split position to another involves not only translations but also rotations. The tensor B is therefore different for different positions. The high-temperature limit of the pseudo potential is then

$$\begin{aligned} PV(x) &= C + \sum_i c_i f_i(\mathbf{x} - \mathbf{x}_i) \\ &= C + \sum_i c_i(\mathbf{x}\mathbf{B}_i\mathbf{x} - 2\mathbf{x}\mathbf{B}_i\mathbf{x}_i + \mathbf{x}_i\mathbf{B}_i\mathbf{x}_i) \\ &= C' + \mathbf{x}(\sum_i c_i\mathbf{B}_i)\mathbf{x} - 2\mathbf{x}\sum_i c_i\mathbf{B}_i\mathbf{x}_i. \end{aligned}$$

In a symmetrical arrangement of split positions the last term in the above formula vanishes and det $(\sum_i c_i B_i) = \det B_i$ for all split positions. The averaging of the B_i leads to a more isotropic B for the pseudo potential.

It is interesting to note that the high-temperature limit of the pseudo potential is harmonic, although the pseudo potential at low temperatures is very anharmonic.

In the anharmonic case the pseudo potential also becomes steeper with increasing temperature. The limit, however, is not equal to the original potential at a split position. This is shown in one dimension with an anharmonic potential expanded in a power series up to the fourth order:

$$V_i(x) = \beta(x - x_i)^2 + \gamma(x - x_i)^3 + \delta(x - x_i)^4.$$

The limit of the pseudo potential then becomes

$$\begin{aligned} PV(x) &= C + \sum_i c_i f_i(x - x_i) \\ &= C + \sum_i c_i[\beta(x - x_i)^2 + \gamma(x - x_i)^3 + \delta(x - x_i)^4] \\ &= C' + \beta x^2 + \gamma x^3 + \delta x^4 \\ &\quad + (3\gamma \sum_i c_i x_i^2 - 4\delta \sum_i c_i x_i^3)x \\ &\quad + 6\delta(\sum_i c_i x_i^2)x^2 \\ &= C' + \gamma x + (\beta + 6\delta \sum_i c_i x_i^2)x^2 + \gamma x^3 + \delta x^4. \end{aligned}$$

This deviation has for $x \simeq x_i$ the same order of magnitude as the contribution of the anharmonic terms to the overall potential. This approximation still gives a reasonable estimate of the original potential compared with the pseudo potential at low temperatures, as long as anharmonic terms are small compared with the harmonic terms, or the split positions are close together.

APPENDIX 3

Temperature dependence of the harmonic temperature factors for different potentials and split positions

If anharmonic deviations of a p.d.f. are described with the Gram-Charlier or the Edgeworth expansion omitting the first two terms, the harmonic temperature factor is proportional to the variance of the p.d.f. or the mean-square displacement from the mean position (Johnson & Levy, 1974). (If coefficients of an expansion of the potential are refined, the harmonic temperature factor gives the curvature.) In the high-temperature limit and for one dimension, temperature factor and potential are related by

$$T_{\text{harm}} \propto \int_{-\infty}^{\infty} x^2 \,\text{pdf}\,(x)\,\mathrm{d}x = \frac{\displaystyle\int_{-\infty}^{\infty} x^2 \exp[-V(x)/kT]\,\mathrm{d}x}{\displaystyle\int_{-\infty}^{\infty} \exp[-V(x)/kT]\,\mathrm{d}x}.$$

This gives for potentials of the form $V(x) = ax^n$ a harmonic temperature factor which is proportional to T^{2n}. In cases where the potential deviates from the harmonic potential only at large x, the harmonic temperature factor rises faster if the potential becomes flatter and more slowly if the potential becomes steeper at high x. Extrapolating these temperature factors to 0 K from a limited temperature range may give high positive or negative intercepts although the harmonic part of the temperature factor goes to 0. Anharmonic potentials with a static temperature factor are given by Mair (1982*b*).

The harmonic temperature factor of split positions in the averaged structure is proportional to the mean-square displacement of an atom from the centre of gravity which is given by the variance of the joint p.d.f. The variance of the joint p.d.f. can be given in terms of the variance of each single p.d.f. and its distance from the centre of gravity:

$$\begin{aligned} \sigma_{ij}^2 &= \int_{-\infty}^{\infty} x_i x_j \,\text{PDF}\,(x)\mathrm{d}^3x \\ &= \sum_n w_n \int_{-\infty}^{\infty} (x_i - x_{ni} - d_{ni}) \\ &\quad \times (x_j - x_{nj} - d_{nj})\,\text{pdf}_n(x)\,\mathrm{d}^3x \\ &= \sum_n w_n \int_{-\infty}^{+\infty} [(x_i - x_{ni})(x_j - x_{ij}) + d_{ni}(x_j - x_{nj}) \\ &\quad + d_{nj}(x_i - x_{ni}) + d_{nj}d_{ni}]\,\text{pdf}_n(x)\,\mathrm{d}^3x \\ &= \sum_n w_n(\sigma_{n,ij}^2 + d_{ni}d_{nj}), \end{aligned}$$

where x_n is the split position n, d_n its vector to the centre of gravity, w_n the occupancy and $\sigma_{n,ij}$ the variance of p.d.f.$_n$. This formula is equal to the one obtained earlier (Schulz, 1972) for the harmonic case.

The variance of the joint p.d.f. can be split into two terms. The first term contains the variances of all positions and depends on temperature, the second contains the distances of the split positions from their centre of gravity and is independent of temperature. This allows the average distance of a split position from the centre of gravity to be determined by extrapolating the harmonic temperature factor to 0 K (assuming the vibrations at 0 K are negligible).

References

Bachmann, R. (1983). *Untersuchung schneller Ionen leiter mit Hilfe elastischer Röntgen- oder Neutronenbeugung.* Thesis, Univ. Karlsruhe, Federal Republic of Germany.

Bachmann, R., Kreuer, K. D., Rabenau, A. & Schulz, H. (1982). *Acta Cryst.* **B38**, 2361–2364.

Bachmann, R. & Schulz, H. (1983). *Solid State Ionics*, **9&10**, 521–524.

Bell, M. F., Breitschwerdt, A. & von Alpen, U. (1981). *Mater. Res. Bull.* **16**, 262–272.

Cava, R. J., Reidinger, F. & Wuensch, B. J. (1977). *Solid. State Commun.* **24**, 411–416.

Dawson, B., Hurley, A. C. & Maslen, V. W. (1967) *Proc. R. Soc. London Ser.* A, **298**, 289–306.

Johnson, C. K. (1970). In *Thermal Neutron Diffraction*, edited by B. T. M. Willis, 132–160. Oxford Univ. Press.

Johnson, C. K. & Levy, H. A. (1974). In *International Tables for X-ray Crystallography*, Vol. IV, 311–336. Birmingham: Kynoch Press.

Kuhs, W. F. (1983). *Acta Cryst.* **A39**, 148–158.

Mair, S. L. (1980). *J. Phys. C*, **13**, 1419–1425.

Mair, S. L. (1982*a*). *J. Phys. C*, **15**, 25–36.

Mair, S. L. (1982*b*). *Acta Cryst.* **A38**, 790–796.

Mair, S. L., Barnea, Z., Cooper, M. J. & Rouse, K. D. (1974). *Acta Cryst.* **A30**, 806–813.

Megaw, H. D. (1968). *Acta Cryst.* **B25**, 1516–1517.

Perenthaler, E. (1981). *Zusammenhang zwischen Ionenleitfähigkeit und Kristallstruktur am Beispiel von* Ag_3SI. Thesis, Univ. Karlsruhe, Federal Republic of Germany.

Perenthaler, E., Schulz, H. & Beyerle, H. U. (1981). *Solid State Ionics*, **5**, 493–496.

Reidinger, F. (1979). *Sodium Beta-Alumina: Structure Analysis of a Superionic Conductor.* Thesis, State Univ. of New York at Albany.

Roberto, J. B., Battermann, B. W., Keating, D. T. (1974). *Phys. Rev. B*, **9**, 2590–2599.

Schulz, H. (1972). *Z. Kristallogr.* **136**, 321–349.

Willis, B. T. M. (1969). *Acta Cryst.* **A25**, 277–300.

Willis, B. T. M. & Pryor, A. W. (1975). *Thermal Vibrations in Crystallography.* Cambridge Univ. Press.

Wittingham, M. S. & Huggins, R. A. (1971). *J. Chem. Phys.* **54**, 414–416.

Zucker, U. H., Perenthaler, E., Kuhs, W. F., Bachmann, R. & Schulz, H. (1983). *J. Appl. Cryst.* **16**, 358.

Zucker, U. H. & Schulz, H. (1982*a*). *Acta Cryst.* **A38**, 563–568.

Zucker, U. H. & Schulz, H. (1982*b*). *Acta Cryst.* **A38**, 568–576.

Acta Cryst. (1984). A**40**, 675-679

Dynamical X-ray Diffraction from Crystals with Precipitates.
I. Theory of the Bragg Case

By V. Holý

Department of Solid State Physics, Faculty of Science, J. E. Purkyně University, Kotlářská 2, 611 37 *Brno, Czechoslovakia*

(*Received* 5 *December* 1983; *accepted* 30 *May* 1984)

Abstract

The optical coherence approach has been used for computing the reflection curves of crystals with spherical precipitates in the Bragg case and the curves were compared with those obtained from the usual kinematical theory. It has been shown that the asymmetry of the curves depends on the sign of the volume change caused by defects. Near their maximum the shape of the curves is not dependent on the type of deformation field of the precipitates and it depends on the properties of the perfect crystal. In comparison with the kinematical theory it has been demonstrated that the difference between the results of the dynamical theory and those of the kinematical theory are significant only near the maximum of the reflection curves.

1. Introduction

In dislocation-free silicon crystals grown by the Czochralski method structural transformations take place during the technological process, namely precipitates of other phases or other microdefects can occur. The defects affect the electrical properties of the semiconductors or they can cause the formation of dislocation loops.

X-ray methods of investigating microdefect formation are advantageous owing to their non-destructivity. The theoretical description of X-ray diffraction from crystals with randomly distributed small defects has been given in the kinematical approximation in the theory of diffuse scattering in papers by Dederichs (1971), Larson & Schmatz (1980) and Trinkaus (1972). The kinematical theory enables us

0108-7673/84/060675-05$01.50